

One probabilistic model designed for a
better understanding of the pluvial
floods, their prediction and promptness
in reactions of the urgent services

Final Version of December/2021

Deliverable number 4.1.3.

Project Acronym	STREAM
Project ID Number	10249186
Project Title	Strategic Development of Flood Management
Priority Axis	2 - Safety and Resilience
Specific objective	2.2 - Increase the safety of the Programme area from natural and man-made disaster
Work Package Number	4
Work Package Title	Development of innovative technologies and system of flood forecasting and early warning system
Activity Number	4.1.
Activity Title	Flood forecasting system
Partner in Charge	CNR - ISMAR
Partners involved	LP, PP3, PP8, PP14, PP15
Status	Final
Distribution	Public

Summary

1	Introduction.....	1
1.1	Background.....	1
1.2	Weather forecasting in Croatia.....	1
1.3	Severe weather warning system in Croatia.....	5
2	Methodology.....	7
2.1	Study area.....	7
2.2	Flooding reports.....	10
2.3	Rainfall data.....	11
2.4	Rainfall threshold approach.....	15
2.5	Machine learning (ML) approach.....	16
2.6	Feature selection.....	17
2.7	Model performance.....	18
3	Early warning system for pluvial flooding.....	19
3.1	Threshold-based EWS.....	19
3.2	Machine-learning EWS.....	21
4	Pluvial flood forecast model.....	26
4.1	Threshold-based pluvial flood forecast.....	26
4.2	ML-based pluvial flood forecast.....	28
5	Conclusion.....	33
	Literature.....	34

Client: **UNIVERSITY OF ZADAR**
Ulica Mihovila Pavlinovića 1
23 000 Zadar



Sveučilište u Zadru
Universitas Studiorum
Jadertina | 1396 | 2002 |

Title: **HYDROLOGICAL-HYDRAULIC ANALYSES WITH
CORRESPONDING MAPS AND FLOOD RISK MANAGEMENT
PLAN**

Documentation type: Study documentation

Contract: University of Zadar (406-01/21-01/145)
University of Rijeka, Faculty of Civil Engineering (361-08/21-01/11)
Vodoprivredno-projekttni biro d.d. (VPB - KUG - 21-0034)
Croatian Meteorological and Hydrological Service (920-08/21-13/14)

Project manager: Assist. Prof. Nino Krvavica, PhD

Contractor: **UNIVERSITY OF RIJEKA, FACULTY OF CIVIL ENGINEERING
VODOPRIVREDNO-PROJEKTNI BIRO d.d.
CROATIAN METEOROLOGICAL AND HYDROLOGICAL SERVICE**

Subcontractor: **CENTAR GRAĐEVINSKOG FAKULTETA d.o.o.**

Place and date: Rijeka - Zagreb, December 2021

Team experts:

Project manager and hydraulic expert:	Assist. Prof. Nino Krvavica, MEng, PhD, (Građevinski fakultet u Rijeci)
Hydrological expert:	Assist. Prof. Josip Rubinić, MEng, PhD (Građevinski fakultet u Rijeci)
Oceanographic expert:	Prof. Goran Lončar, MEng, PhD (Centar Građevinskog fakulteta d.o.o.)
Flood risk management expert	Ana Jelka Graf, MEng (Vodoprivredno-projektni biro d.d.)
Consultant for flood modelling:	Dario Kolarić, MEng (Vodoprivredno-projektni biro d.d.)
Water quality expert:	Neven Cukrov, PhD (Institut Ruđer Bošković)
Climatology expert:	Ksenija Cindrić Kalin, PhD (Državni hidrometeorološki zavod)
Sustainable urban drainage system expert:	Tatjana Uzelac, MEng (Starum d.o.o.)

KLASA: 361-08/21-01/11

URBROJ: 2170-57-05-00-21-7

Client: **UNIVERSITY OF ZADAR**
Ulica Mihovila Pavlinovića 1, 23 000 Zadar

Contractor: **UNIVERSITY OF RIJEKA, FACULTY OF CIVIL ENGINEERING**
VODOPRIVREDNO-PROJEKTNI BIRO d.d.
CROATIAN METEOROLOGICAL AND HYDROLOGICAL SERVICE

Subcontractor: **CENTAR GRAĐEVINSKOG FAKULTETA d.o.o.**

**PROBABILISTIC MODEL DESIGNED FOR BETTER
UNDERSTANDING THE PLUVIAL FLOODS, ITS
PREDICTION AND PROMPTNESS IN REACTIONS OF
URGENT SERVICES**

Document Nr.: 033/2021

Project manager: **Nino Krvavica, PhD**

Project manager:

Dean:

Nino Krvavica, PhD

Mladen Bulić, PhD

Title: HYDROLOGICAL-HYDRAULIC ANALYSES WITH
CORRESPONDING MAPS AND FLOOD RISK MANAGEMENT
PLAN
Probabilistic model designed for better understanding the pluvial
floods, its prediction and promptness in reactions of urgent services

Client: UNIVERSITY OF ZADAR
Ulica Mihovila Pavlinovića 1, 23 000 Zadar

Contractor: UNIVERSITY OF RIJEKA, FACULTY OF CIVIL ENGINEERING
VODOPRIVREDNO-PROJEKTNI BIRO d.d.
CROATIAN METEOROLOGICAL AND HYDROLOGICAL SERVICE

Project manager: Assist. Prof. Nino Krvavica, MEng, PhD

Team:

University of Rijeka Assist. Prof. Bojana Horvat, MEng, PhD
Assist. Prof. Igor Ružić, MEng, PhD

Croatian Meteorological and Hydrological Service Ksenija Cindrić Kalin, PhD
Leonardo Patalen, MEng
Davor Nikolić, MEng
Ivana Marinović, MEng



1 Introduction

1.1 Background

One of the goals of the STREAM project is to create new forecasting system for pluvial floods in Croatia. One of the project assignments is to perform a detailed analysis of urban flooding in the Zadar pilot area and improve the flood forecast system. Specifically, this is planned to be achieved by developing a pluvial flood forecast system for better understanding the pluvial floods, its prediction and promptness in reactions of urgent services.

Therefore, the main aim of this report (study) is to develop a pluvial flood forecast model for the urban area in the Zadar pilot area. The forecast model is based on a 20-year of collected data from news reports and continuous high-resolution rain gauge data. In the following sections, we give a short overview of the operational weather forecasting and severe weather warning system in Croatia. Next, we describe the methodology for developing the forecast system based on rainfall threshold curves and machine-learning (ML) approaches. In the analysis we focus on a better understanding of pluvial floods in Zadar and develop models for an early warning system and pluvial flood forecast system. Finally, we present the model results and give recommendations on the best approaches.

1.2 Weather forecasting in Croatia

Aire Limitée Adaptation dynamique Développement InterNational (ALADIN) is a numerical (computational) model system for short-term high-resolution weather forecasting. Croatia has been a member of the ALADIN cooperation program since 1995, and the forecast of the Croatian version (ALADIN-HR) has been prepared by the Croatian Meteorological and Hydrological Service (DHMZ) since 2000. More about the ALADIN collaboration project can be found on the official ALADIN Consortium web page (<http://www.umr-cnrm.fr/aladin/spip.php?article36>).

The main goal of the ALADIN cooperation project is to improve the forecast of severe weather conditions with an emphasis on the early warning system (EWS) of meteorological and hydrological disasters. Furthermore, timely delivery of prognostic products to end users is important, considering their specific needs (<https://meteo.hr/>).

At DHMZ, there are several operating configurations of ALADIN-HR models that differ primarily in the resolution of the model grid. All configurations are adapted to the weather and climate of Croatia.

Some of the basic features of these operating configurations are (<https://meteo.hr/>):

- horizontal resolution of 4 km and 2 km
- hourly availability of prognostic products up to 72 hours in advance
- new forecast every 6 hours

All forecasts by the ALADIN-HR model are operatively made on the DHMZ supercomputer. In order to calculate the forecast for the next few days with a numerical model, it is necessary to know in advance the current state of the atmosphere, ie. the initial conditions determined by the data assimilation method. Numerous meteorological measurements and observations over Croatia and surrounding countries are used in the data assimilation process: ground measurements (at 2 m and 10 m), aircraft measurements, measurements of polar and geostationary satellites and meteorological balloon measurements (radio sounding measurements). As the ALADIN-HR model has a limited space for forecasting, the calculation also requires meteorological conditions outside its domain (boundary conditions) obtained from the IFS global forecasting model of the European Center for Medium-Range Weather Forecasts (ECMWF).

By increasing the resolution of the model, it is possible to predict the state of the atmosphere more accurately and in more detail. Figure 1.2.1 shows the areas (domains) for which the ALADIN-HR model forecast is calculated and the vertical section through the Velebit mountain for two model configurations at different horizontal resolutions. As can be seen from the figure, the finer resolution of the model provides a more accurate description of the orography and allows a much better forecast of orographic affected processes (eg. wind forecast). Similarly, higher model resolution better represents other physical processes in the model.

ALADIN model products include (<https://meteo.hr/>):

- prognostic maps of meteorological fields at the ground and at vertical levels to the top of the stratosphere
- spatial and temporal vertical cross-sections of meteorological parameters
- meteograms (time courses of meteorological parameters)
- ASCII files, XML and tables of predicted sizes
- GRIB files of forecast fields.

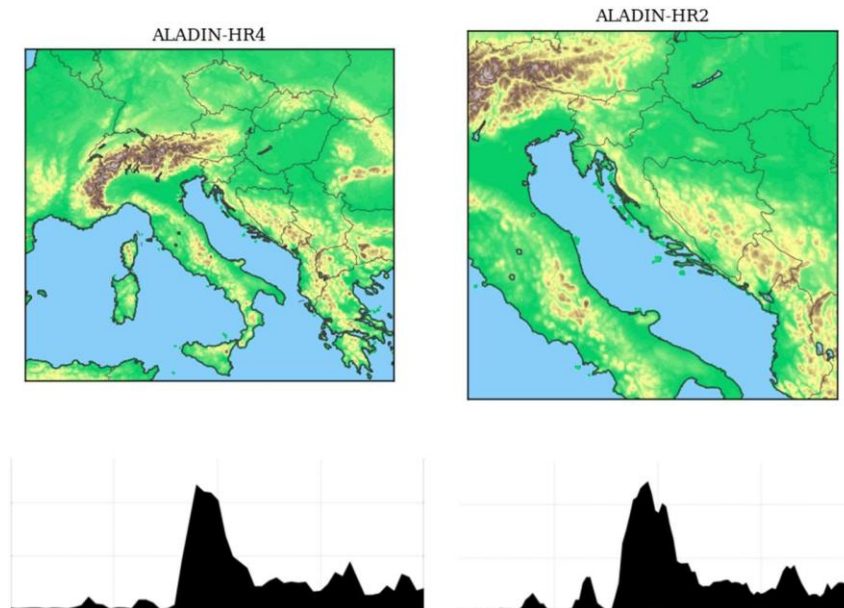


Figure 1.2.1. Areas (domains) for which the ALADIN-HR forecast is calculated and a vertical section through the Velebit mountain for two model configurations at different horizontal resolutions, 4 km and 2 km (<https://meteo.hr/>).

DHMZ issues reports on future weather conditions (weather forecast) based on ALADIN-HR forecast products that are of public and state interest (<https://meteo.hr/>):

- special warnings of dangerous weather conditions
- general weather forecast
- biometeorological forecast.

Specialized forecasts of ALADIN-HR models are issued to users for the needs of (<https://meteo.hr/>):

- ensuring the safety of air, sea, road, and rail transport
- agricultural production and fisheries
- open fire protection
- planning of energy consumption and production of energy from renewable sources (wind, solar, hydropower)
- optimization of business activities in the energy market
- planning outdoor activities (construction works, cultural and sporting events, etc.).

The following ALADIN-HR products are publicly available on the DHMZ website 72 hours in advance with a 3-hour resolution:

- ALADIN maps (example shown in Figure 1.2.2.)
- ALADIN meteograms (example shown in Figure 1.2.3)

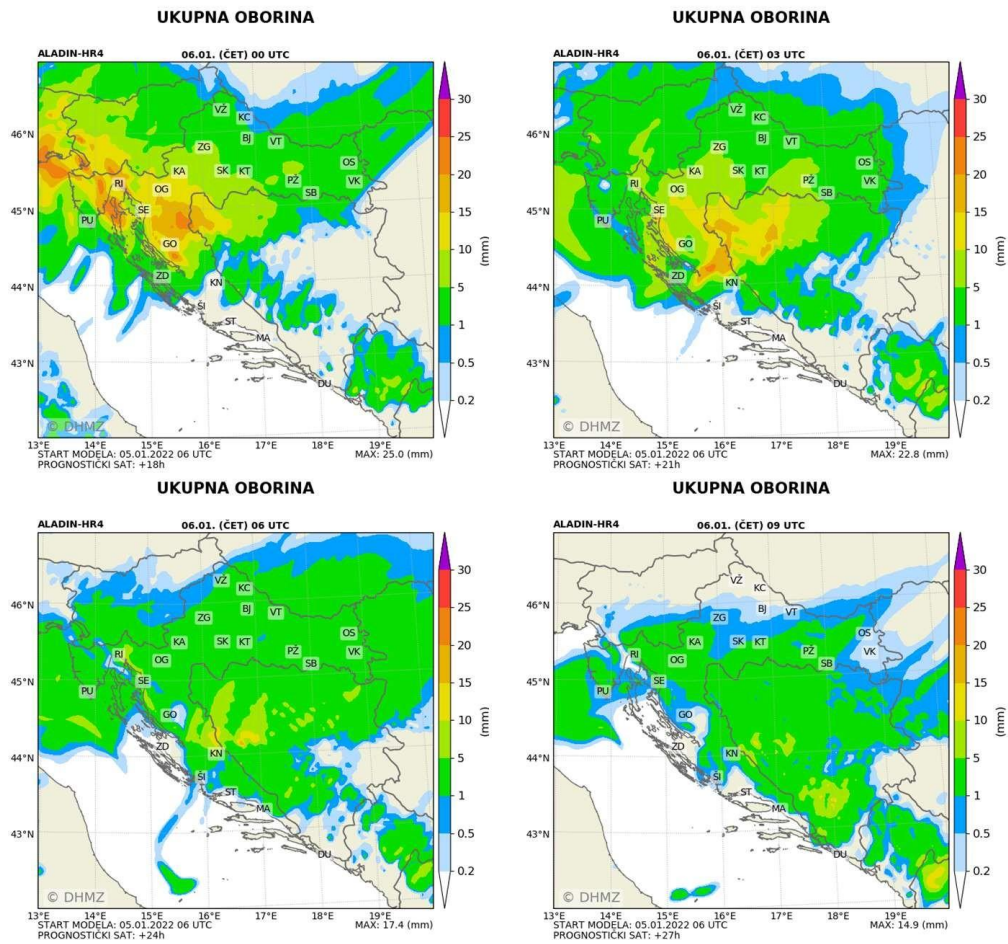


Figure 1.2.2. Example of ALADIN forecast maps for precipitation (hrv. *ukupna oborina*)

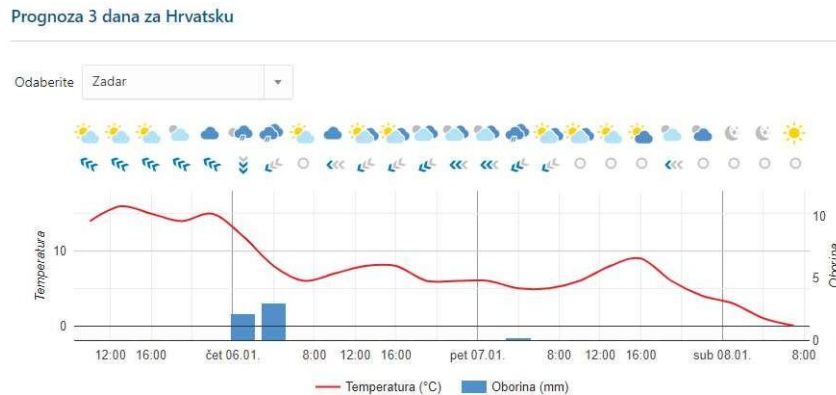


Figure 1.2.3. Example of ALADIN meteogram for Zadar, showing temperature (hrv. *temperatura*) and precipitation (hrv. *oborina*) for city of Zadar

1.3 Severe weather warning system in Croatia

The Croatian Meteorological and Hydrological Service (DHMZ) provides Early Warning Systems for the natural hazards in Croatia for (www.meteo.hr):

- Severe weather conditions (severe wind, heat wave warning, cold wave warning, intensive precipitations, phenomena like snow, black ice, poor visibility)
- Severe flooding conditions (at river basins, for flash floods)
- Drought prediction
- Severe marine meteorological conditions (wind, sea state, thunderstorms and visibility) 4 times daily for the following 24 hours available for the public, plus 3-day outlook twice daily only for authorities and special users.

The severe weather warning system is integrated with METEOALARM (<https://meteoalarm.org/>), which integrates all important severe weather information originating from the official National Public Weather Services across many European countries. This information is presented consistently to ensure coherent interpretation as widely as possible throughout Europe.

METEOALARM is easily accessible to the public, simple and understandable to everyone. Using symbols and color-coded maps, it provides the most recent warnings of expected dangerous weather for the next 48 hours in much of Europe. Warnings are given for the following phenomena: heavy rain with the possibility of flooding, intense thunderstorms, stormy winds, heat waves, forest fires, fog, snow or extreme cold with blizzards, avalanches, and high coastal tides.

The colours on the coded map represent four levels of warning: red indicates the greatest danger of dangerous weather conditions, followed by orange and yellow, and green means that dangerous weather is not expected (www.meteo.hr). In Croatia, the sub-daily time scale (6 hours and 12 hours) is used to select an appropriate threshold value to define yellow, green, and red alarming categories for extreme rainfall events in the Meteoalarm rainfall warning system (Cindrić Kalin et al., 2021.). Furthermore, the country is divided into 8 land regions and 6 sea regions. An example of severe weather warnings in Croatia is illustrated in Figure 1.3.1.

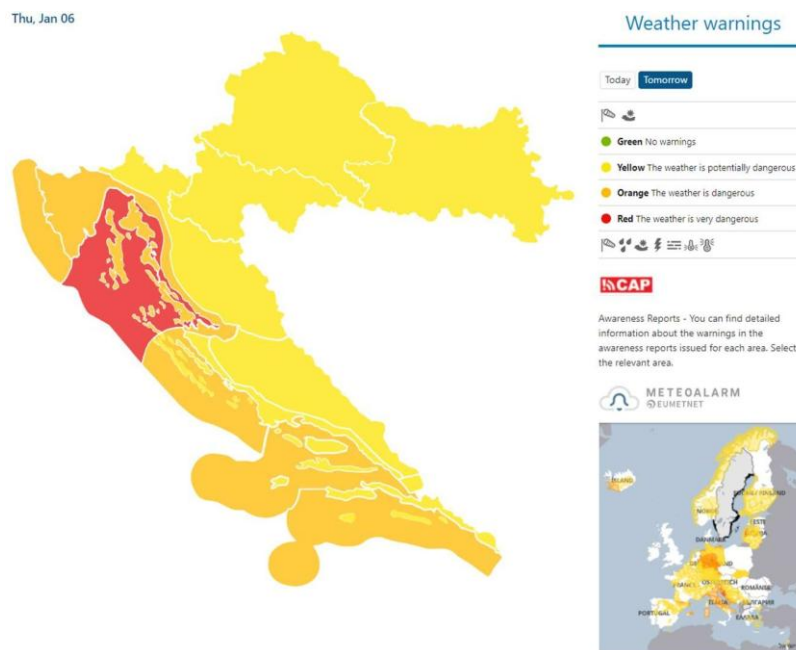


Figure 1.3.1. Example of severe weather warnings by the Croatian Meteorological and Hydrological Service (<https://meteo.hr/naslovnica-upozorenja.php?lang=en&tab=upozorenja>)

Croatian Meteorological and Hydrological Service (DHMZ) disseminates forecasts to Main (National) Flood Protection Centre and other interested parties as well as to the public through multiple channels such as WEB, FTP, TV forecasts etc. The main (National) Flood Protection Centre compiles information received, with other relevant information such as daily and hourly recorded water levels, water flows, precipitation, temperatures, hydrological forecasts etc in a daily report which is delivered to parties and persons involved in operative flood defence in Croatia, and if needed to flood protection administrations of neighbouring countries and the public.

2 Methodology

2.1 Study area

The city of Zadar is situated on the eastern coast of the Adriatic Sea. The city covers 25 km² with a population of 75,082 (2011 census), which makes it the second-largest city of the Dalmatia region and the fifth-largest city in Croatia. Zadar has a borderline humid subtropical (Cfa) and Mediterranean climate (Csa), with mild, wet winters and very warm, humid summers.

Short high-intensity rainfall is the main cause of pluvial flooding in the Zadar pilot area. On September 11, 2017, extremely large amounts of rainfall caused pluvial and flash floods in Zadar with significant material damage. Between Sunday evening (10 Sept) and Monday evening (11 Sep) 285 mm of rain was measured in Zadar, and around 325 mm at Zadar airport, Zemunik. Figure 2.1.1 shows several news photographs from this extreme flood event.



Figure 2.1.1. Photographs from the September 2017 flood in Zadar (zadarski.slobodnadalmacija.hr)

The land cover in the Zadar catchment is shown in Figure 2.1.2, based on Urban Atlas (Copernicus Land Monitoring Services). The main characteristic of the catchment is illustrated in Figure 2.1.3., which shows the digital elevation model, drainage network (SAGA channels), imperviousness density (Copernicus Land Monitoring Services) and population density (Worldpop, 2018). The city centre is located near the coast, with a high percentage of impervious area and dens population, making it prone to pluvial flood hazards, as well as exposed to pluvial flood risks.

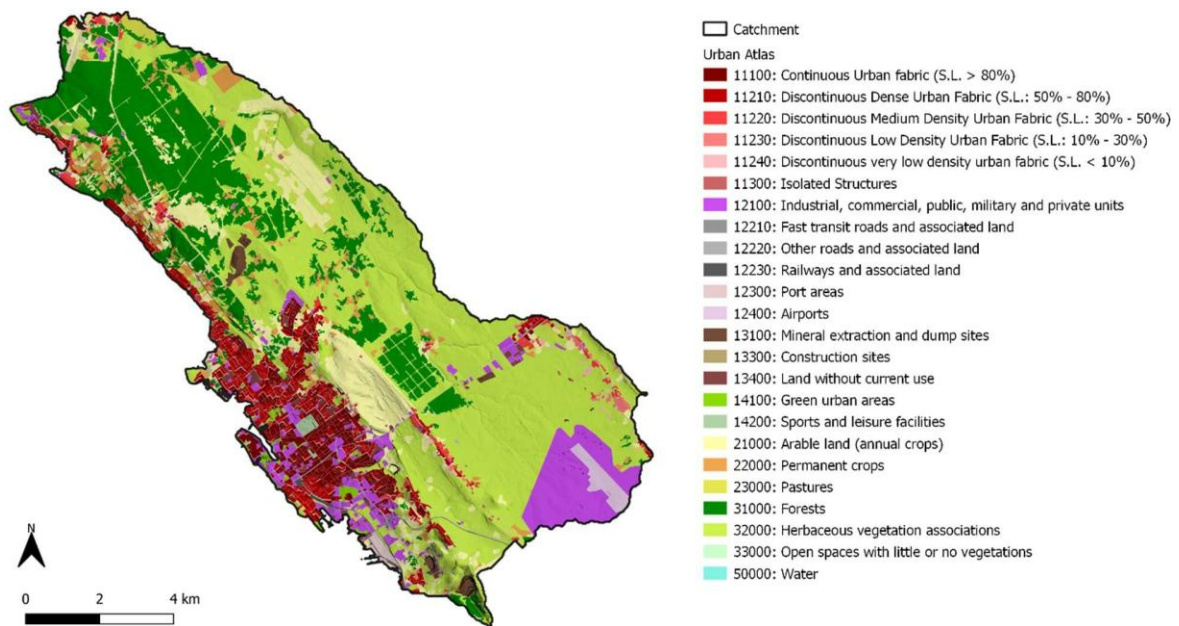


Figure 2.1.2. Zadar pilot area land cover (Urban Atlas, Copernicus)

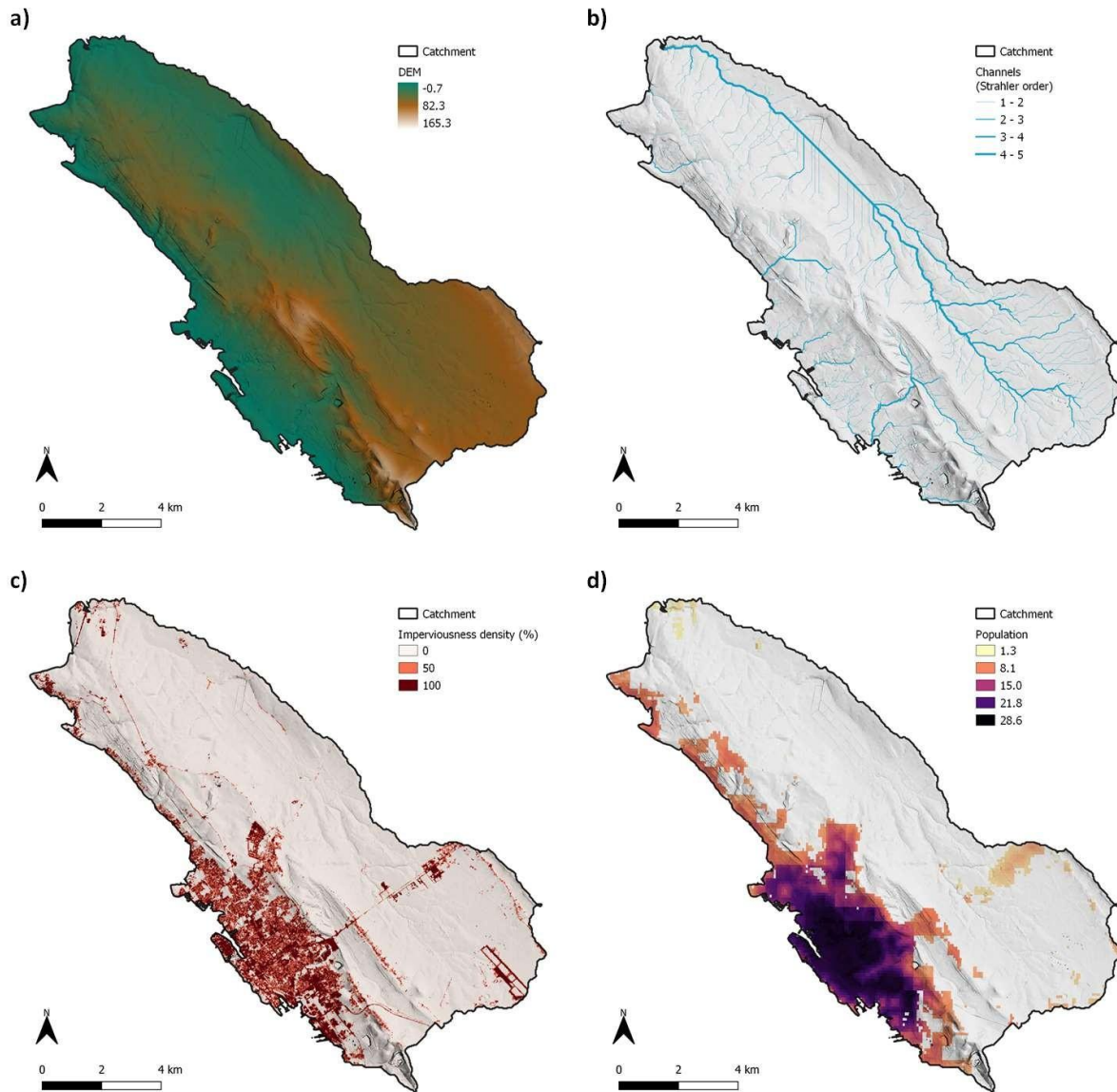


Figure 2.1.3. Zadar pilot area catchment characteristics: a) Digital elevation model (DEM), b) Drainage network (SAGA channels), c) Imperviousness density (Copernicus), d) Population density (Worldpop).

2.3 Rainfall data

Rainfall at the Zadar pilot area is measured by the official rain gauge (pluviograph) at meteorological station Zadar, with a 5 min temporal resolution. For this study, we used a continuous time series of 5-min rainfall depth from the period 2000-2020. The rainfall depths were aggregated to longer time scales (hourly, daily, and monthly) for a preliminary analysis.

Figure 2.3.1 shows the monthly, daily, and hourly rainfall inter-annual statistics, as well as the number of flooding and non-flooding events in Zadar. The maximum and mean monthly rainfall during the year is shown in Figure 2.3.1a., which shows that the mean monthly rainfall usually occurs in the autumn months (Sep – Nov), whereas the maximum rainfall usually occurs in the summer and autumn months (Jul, Sep and Oct).

Maximum 24-hour rainfall measured in the period 2000-2020 is shown in Figure 2.3.1b. These values are equally distributed throughout the year, except for a single extreme event (a huge mesoscale convective system), which occurred on 11 September 2017 and caused extensive pluvial and flash floods, widespread material damage and even jeopardised human lives (<https://www.eumetsat.int/flash-floods-zadar-and-surrounding-areas>). Maximum short-term 1-hour rainfall (Figure 2.3.1d.), on the other hand, usually occurs in the summer and autumn months (Jul, Sep and Oct), which correlates with maximum monthly rainfall.

Finally, Figure 2.3.1c shows the inter-annual distribution of non-flooding and flooding events. This figure shows that the largest number of rainfall events occur in the autumn and winter months (from Sep to Feb), however, the largest number of flooding events occurs in the summer and autumn months (Aug, Sep, Oct, and Nov), which correlates with the maximum 1-hour rainfall.

The rainfall data were pre-processed for further (flood forecast) analysis. First, the individual rainfall events were identified based on the condition of a 12-hour no-rain period between two events. Then significant rainfall events were selected from the set that had > 10 mm of rain in a 24-hour period. This procedure resulted in 565 significant individual rainfall events out of 1456 total rainfalls that occurred from 2000 to 2020. Figure 2.3.2. shows all and selected rainfalls given their duration and total depth (Figure 2.3.2c) with corresponding rainfall duration histograms (Figure 2.3.2a, b). Notice that rainfall durations range from 1 hr to 6 days, although most frequent events last from 6 to 12 hours. One event that stands out with almost 300 mm of rainfall in less than 40 hours is the extreme flood from September 2017, mentioned previously.

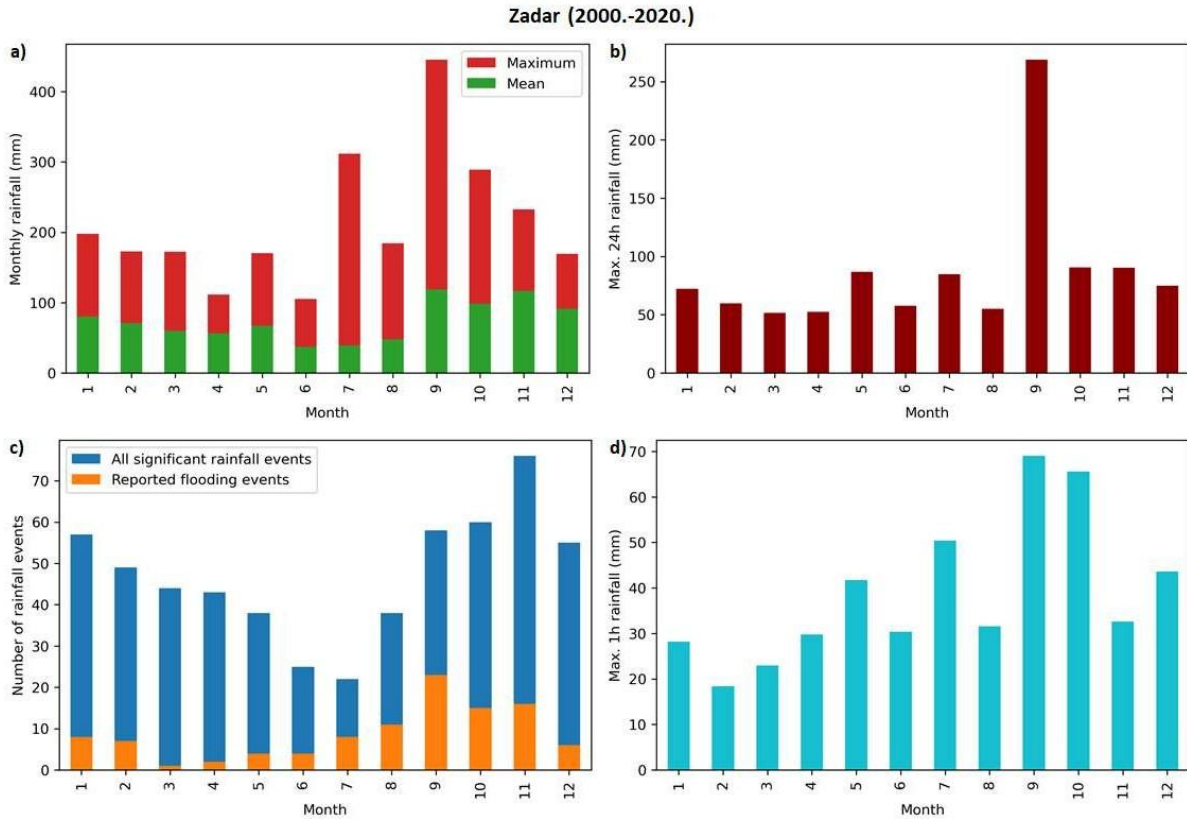


Figure 2.3.1. Inter-annual rainfall statistics in Zadar (2000-2020): a) mean and maximum monthly rainfall, b) maximum daily rainfall, c) number of flooding and non-flooding events, and d) maximum 1-hour rainfall.

For each selected rainfall event, the maximum rainfall depth $H_{\max}(t)$ at every considered duration t (temporal scale) was computed using the following expression:

$$H_{\max}(t) = \max_j \left\{ \sum_{k=1}^{t/5} H_5(k), \dots, \sum_{k=1+j}^{t/5+j} H_5(k), \dots, \sum_{k=1+(1440-t)/5}^{1440/5} H_5(k) \right\} \quad (1)$$

where $j = 0, 1, \dots, N$, with $N = (1400-t)/5$ is the number of aggregated rainfall depths for each duration, H_5 is 5-min rainfall depth, and $t = 10, 30, 60, 120, 180, 240, 360, 540, 720$ and 1440 min are all rainfall durations considered in this analysis. Note that each item in the bracket of Eq. (1) represents a t -min rainfall depth accumulated from k 5-min rainfall depths, and H_t is then the maximum value of all accumulated rainfalls for a selected duration.

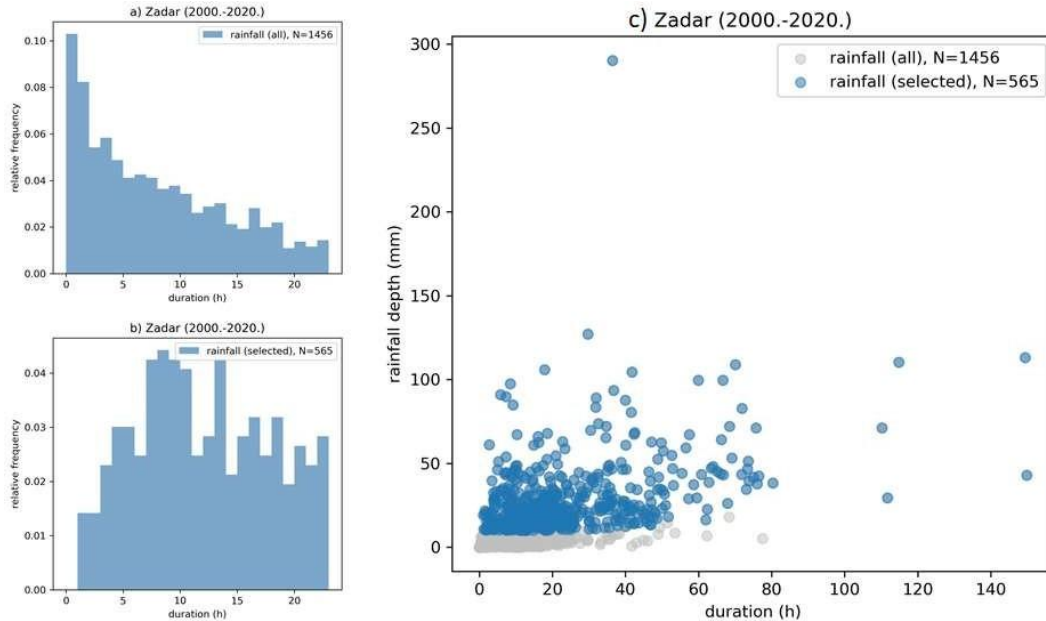


Figure 2.3.2. Individual rainfall events in Zadar (2000-2020): a) duration histogram for all rainfall events, b) duration histogram for significant (selected) rainfall events, and c) total rainfall depth vs duration for all and selected rainfall events.

Figure 2.3.3 shows depth-duration curves for all selected rainfall events classified as either *flooding* or *non-flooding* events based on collected and processed news reports. The main challenge with classifying these events based on rainfall depths is the high percentage of overlap for all considered durations. This is additionally illustrated in Figure 2.3.4 by histograms of rainfall depths for a representative short duration (1 hour) and a long duration (24 hours). This figure suggests that both flooding and non-flooding events can occur when the 1-hour rainfall is in the range of 0-30 mm, and 24-hour rainfall depth is in the range of 20-50 mm, which makes it difficult to directly select an appropriate rainfall depth threshold. Therefore, a more careful analysis is required.

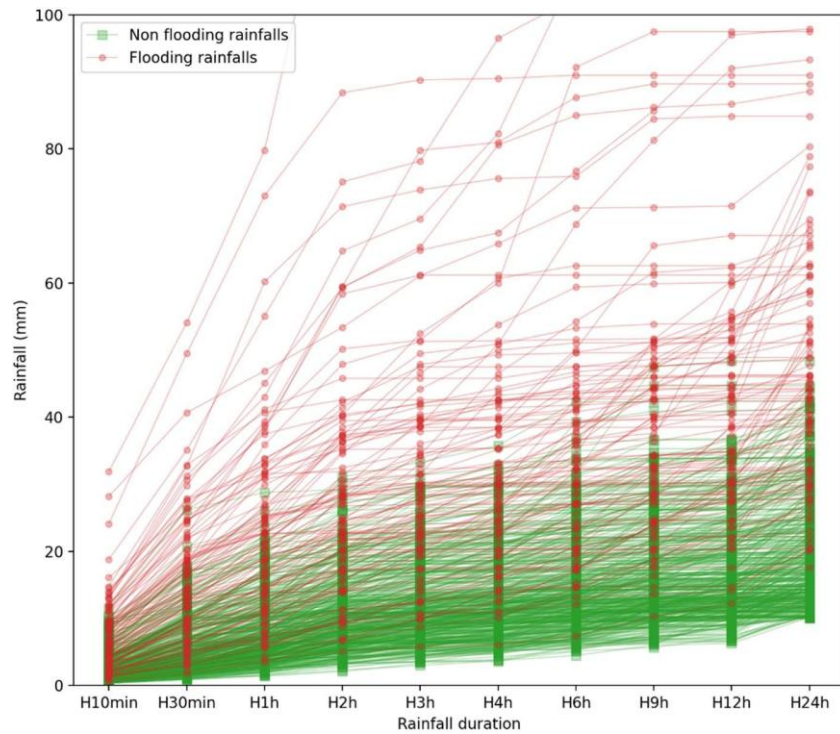


Figure 2.3.3. Depth duration curves for all considered rainfall events classified as flooding and non-flooding events based on news reports.

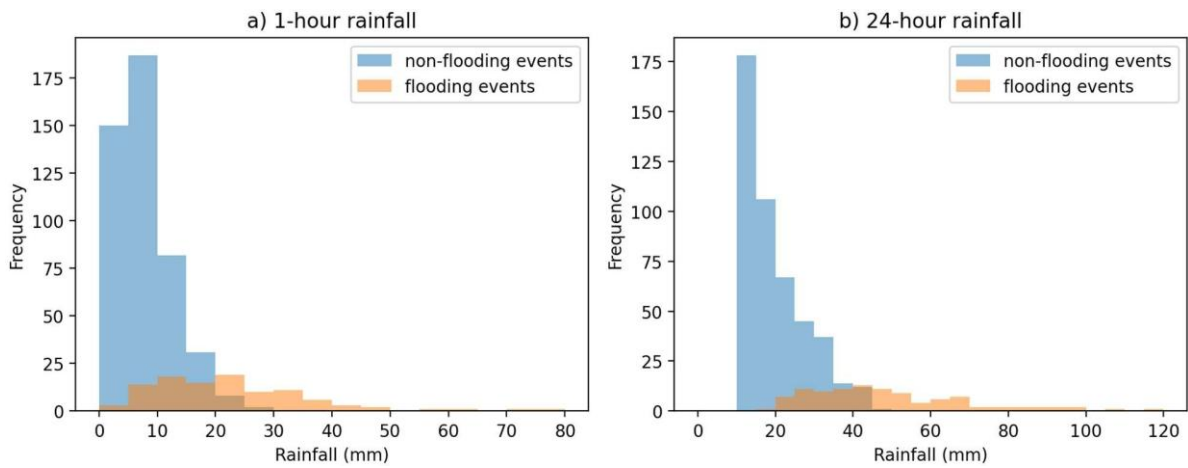


Figure 2.3.4. Histogram of flooding and non-flooding rainfall depths for 1-hour and 24-hour durations

2.4 Rainfall threshold approach

A conventional and simple approach for flood forecast is a rainfall threshold (Martina et al., 2006; Yang et al., 2016; Tian et al., 2019; Ke et al., 2020). Specifically, a rainfall threshold is defined by a single rainfall depth (so-called *critical rainfall threshold*) or several rainfall depths over different time scales or durations (so-called *rainfall threshold curve*), above which a flood is likely to occur (Ke et al., 2020). Rainfall threshold approach is widely used to predict landslides (Giannecchini et al., 2012; Hong et al., 2018), debris flows (Pan et al., 2018) and flash floods (Zhai et al., 2018). The threshold-based approach for flood alerts is based on defining a threshold curve, observing accumulated rainfall and/or rainfall forecast, and issuing a flood alert if the observed/forecasted rainfall exceeds the threshold curve (Figure 2.4.1.).

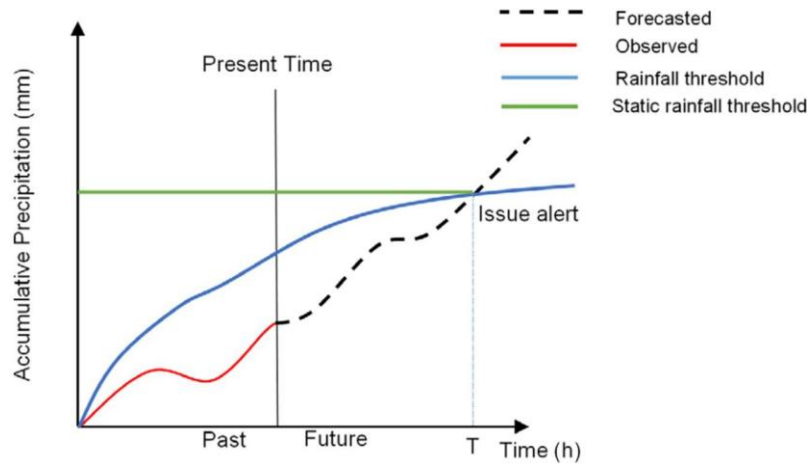


Figure 2.4.1. Threshold-based approach for flood alerts (Young et al., 2021.)

In this study, we follow the approach proposed by Ke et al. (2020) for predicting pluvial flooding with some minor modifications. The threshold curve is defined by maximum (accumulated) rainfall depths for each rainfall duration. Note that these are not cumulative rainfall curves, but maximum depths per each duration (similar to traditional depth-duration-frequency curves). Furthermore, we assume that when the observed maximum rainfall of any considered duration exceeds the threshold, flooding is expected to occur. The flow chart with the main steps for estimating the rainfall threshold curve is shown in Figure 2.4.2. Specifically, in the present analysis, parameters α and β ranged from 0.0 – 0.5 and 0.5 – 1.0, respectively, whereas γ ranged from 0.0 – 1.0.

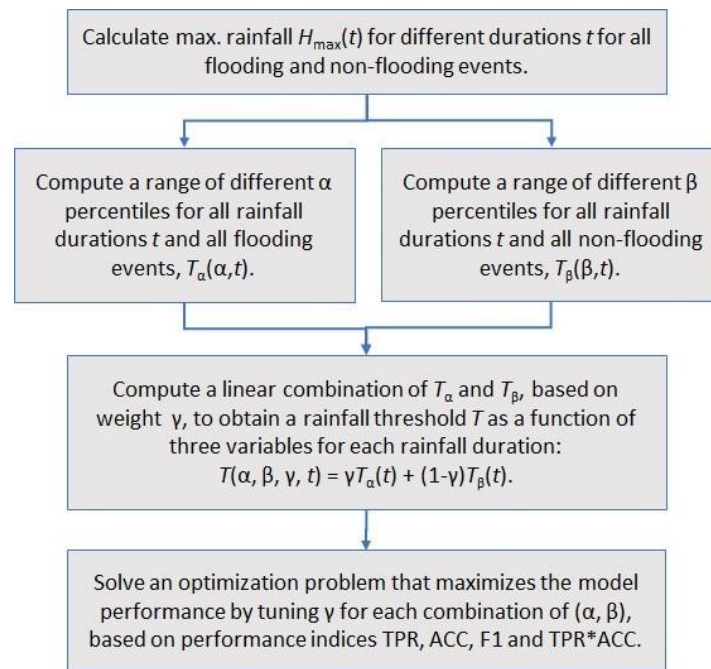


Figure 2.4.2. Flow chart for estimating a rainfall threshold curve for pluvial flooding (modified from Ke et al., 2020.)

2.5 Machine learning (ML) approach

Machine learning (ML) methods, in particular supervised learning methods, are data-driven algorithms that are trained on a subset of available data and then tested on a different subset of data to validate their performance for future inputs. In general, supervised ML are used for classification (identifying which category an object belongs to) or regression problems (predicting a continuous-value attribute associated with an object). The task of flood forecasting is a typical classification problem – identifying if individual rainfall (or a wider set of hydrological variables) belongs to a “flooding” or “non-flooding” category. Given the size of data (rainfall events) and binary outcome, we chose and tested the performance of 10 classification ML algorithms from five major ML categories: a) linear models, b) support vector machines (SVM), c) discriminant analysis, d) decision trees, and e) nearest neighbours (NN) (see Table 2.5.1). All ML algorithms were implemented in Python 3.7 using *scikit-learn* (Pedragosa et al., 2011.).

Table 2.5.1. Machine learning methods applied in this study for predicting pluvial flooding.

Nr.	Category	Model	Parameters
0	Linear models	Logistic regression	No penalty
1	Support Vector Machines	Support Vector Classification	Linear kernel
2		Support Vector Classification	Quadratic kernel
3		Support Vector Classification	Cubic kernel
4	Discriminant analysis	Linear Discriminant Analysis	SVD solver
5		Quadratic Discriminant Analysis	-
6	Decision trees	Decision Tree Classifier	8 leaf nodes
7		Decision Tree Classifier	18 leaf nodes
8	Nearest neighbours	k-neighbours classification	3 neighbours
9		k-neighbours classification	Euclidian distance weight 15 neighbours

2.6 Feature selection

In this study we consider two levels of model operation (purpose) – the first is an early warning system (EWC) for pluvial flooding based on real-time rainfall observations, and the second one is a flood forecasting system based on weather forecasts. Furthermore, for the rainfall threshold curve, only the rainfall depths are considered, whereas for the ML approach we also include air temperature and antecedent rainfall conditions. Since forecasts in Croatia from the ALADIN model are publicly available only in 3h times steps, for forecast models we consider only the 3, 6, 12 and 24-hour rainfalls. Overall, all considered meteorological parameters for each purpose and approach are listed in Table 2.6.1.

For all considered approaches, the dataset was split to training and testing subsets with the ratio 70:30, resulting in 395 events for training and 170 events for testing.

Table 2.6.1. Considered model features for each purpose (EWC or forecast) and each approach (threshold curve and ML)

Variable	Description	EWC		Forecast	
		Threshold curve	ML	Threshold curve	ML
A5d	Antecedent 5-day rainfall (mm)	✗	✓	✗	✗
A15d	Antecedent 15-day rainfall (mm)	✗	✓	✗	✗
A30d	Antecedent 30-day rainfall (mm)	✗	✓	✗	✗

H10min	Maximum 10-min rainfall (mm)	✓	✓	✗	✗
H30min	Maximum 30-min rainfall (mm)	✓	✓	✗	✗
H1h	Maximum 1-hour rainfall (mm)	✓	✓	✗	✗
H2h	Maximum 2-hour rainfall (mm)	✓	✓	✗	✗
H3h	Maximum 3-hour rainfall (mm)	✓	✓	✓	✓
H4h	Maximum 4-hour rainfall (mm)	✓	✓	✗	✗
H6h	Maximum 6-hour rainfall (mm)	✓	✓	✓	✓
H9h	Maximum 9-hour rainfall (mm)	✓	✓	✗	✗
H12h	Maximum 12-hour rainfall (mm)	✓	✓	✓	✓
H24h	Maximum 24-hour rainfall (mm)	✓	✓	✓	✓
Temp	Mean daily air temperature (°C)	✗	✗	✗	✗
		N=10	N=14	N=4	N=4

2.7 Model performance

The performance of all considered models under both approaches were evaluated by several indicators. Since this is a binary classification problem, only four possible outcomes are expected:

- true positive (**TP**) – a flooding event was correctly identified by the model (*hit*)
- true negative (**TN**) – a non-flooding event was correctly identified by the model (*no event*)
- false positive (**FP**) – a non-flooding event was misidentified as a flooding event by the model (*false alarm*)
- false negative (**FN**) – a flooding event was misidentified as a non-flooding event by the model (*miss*)

Based on the number of these four outcomes several indicators are computed, namely:

- True positive rate (recall) **TPR** = $TP / (TP + FN)$
- True negative rate **TNR** = $TN / (TN + FP)$
- Positive predictive rate (precision) **PPR** = $TP / (TP + FP)$
- Negative predictive rate **NPR** = $TN / (TN + FN)$
- Accuracy **ACC** = $(TN + TP) / (TN + TP + FN + FP)$
- F1 score **F1** = $2 * (TPR * PPR) / (TPR + PPR)$

In addition to these traditional scoring indicators, we also considered a product of TPR and ACC as a combined measure of accuracy and recall (TPR_ACC).

3 Early warning system for pluvial flooding

3.1 Threshold-based EWS

Using the training set that consists of 319 non-flooding events and 76 flooding events we performed a thorough search for all possible combinations of parameters α , β and γ . From the pool of several thousand combinations, we selected the three best threshold curves, which have the highest value of at least one of the considered metrics. Derived rainfall thresholds for each considered duration (model feature) are shown in Table 3.1.1. These threshold curves were then applied to the testing set that consists of 141 non-flooding and 29 flooding events. The confusion matrix for each of the three threshold curves is shown in Figure 3.1.1. and performance indicators are given in Table 3.1.2. Finally, the comparison of testing depth-duration curves (flooding and non-flooding) against three derived threshold curves is illustrated in Figure 3.1.2.

All three curves have an accuracy between 0.88 and 0.93 (Table 3.1.2). Curve nr. 0 has the highest overall accuracy, but fewer true positive predictions and a high number of false negative predictions (missed flood events), whereas curve nr. 2 has the highest true positive rate and most true positive predictions, but also a larger number of false positive predictions (false alarms). Curve nr.1 is in between the other two curves with the highest F1 score and balanced false positive and false negative predictions.

Table 3.1.1. Best-performing rainfall thresholds curves in (mm) based on 10 features.

Curve	H10min	H30min	H1h	H2h	H3h	H4h	H6h	H9h	H12h	H24h
0	11.5	26.2	28.8	31.1	33.3	35.8	42.3	44.7	44.7	44.7
1	9.9	22.7	25.2	27.4	29.7	32.0	37.9	40.2	40.4	41.1
2	6.8	15.7	18.0	20.1	22.5	24.4	29.0	31.3	31.7	33.8

Table 3.1.2. Best-performing rainfall threshold curve parameters and their performance indicators based on 10 features.

Curve	α	β	γ	TPR	TNR	PPR	NPR	ACC	F1	TPR_ACC
0	0.0	1.0	0	0.62	0.99	0.95	0.93	0.93	0.75	0.58
1	0.02	1.0	0.15	0.72	0.97	0.84	0.94	0.93	0.78	0.67
2	0.02	1.0	0.45	0.93	0.87	0.60	0.98	0.88	0.73	0.82

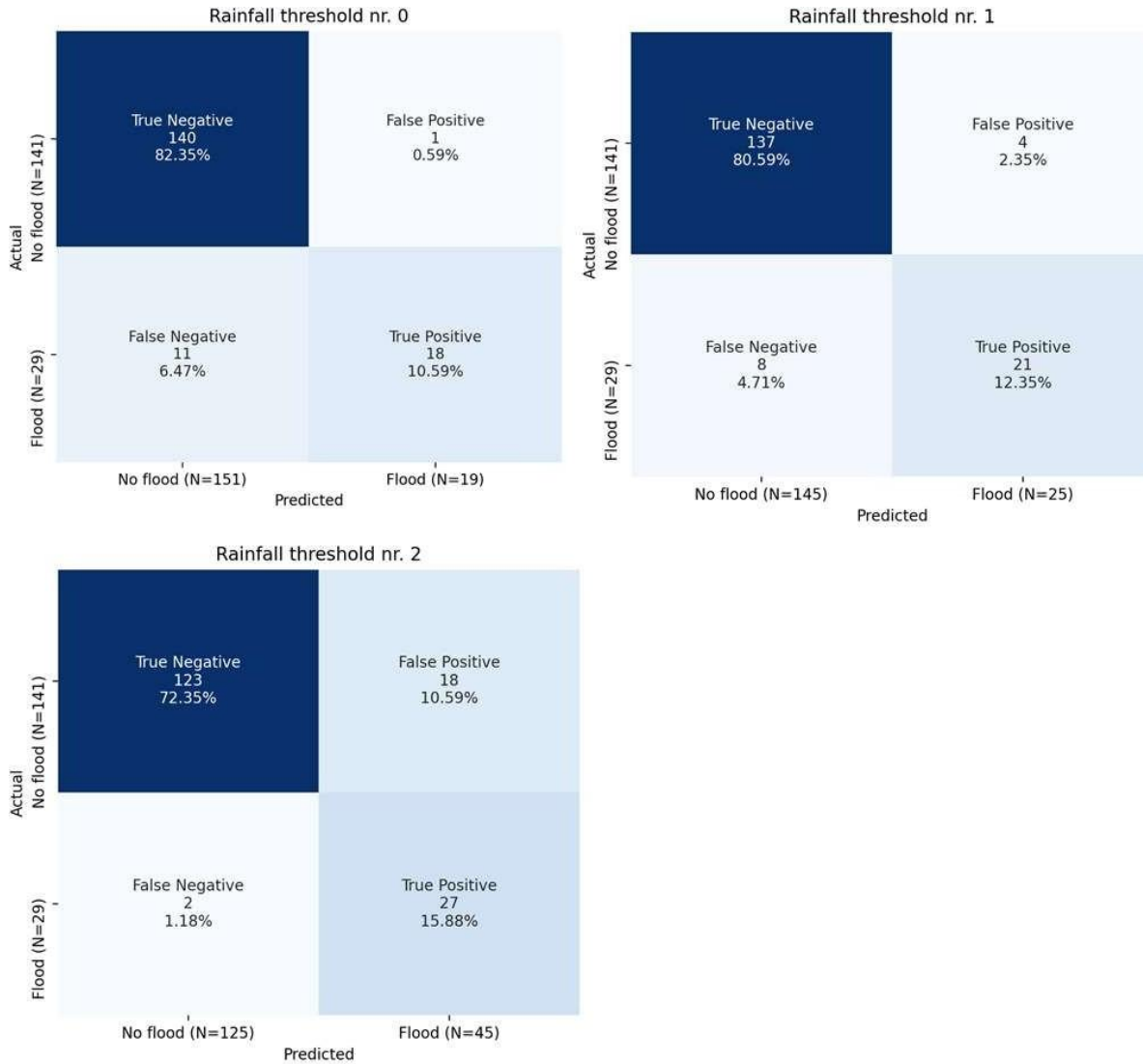


Figure 3.1.1. Confusion matrices for three best performing rainfall threshold curves based on 10 features.

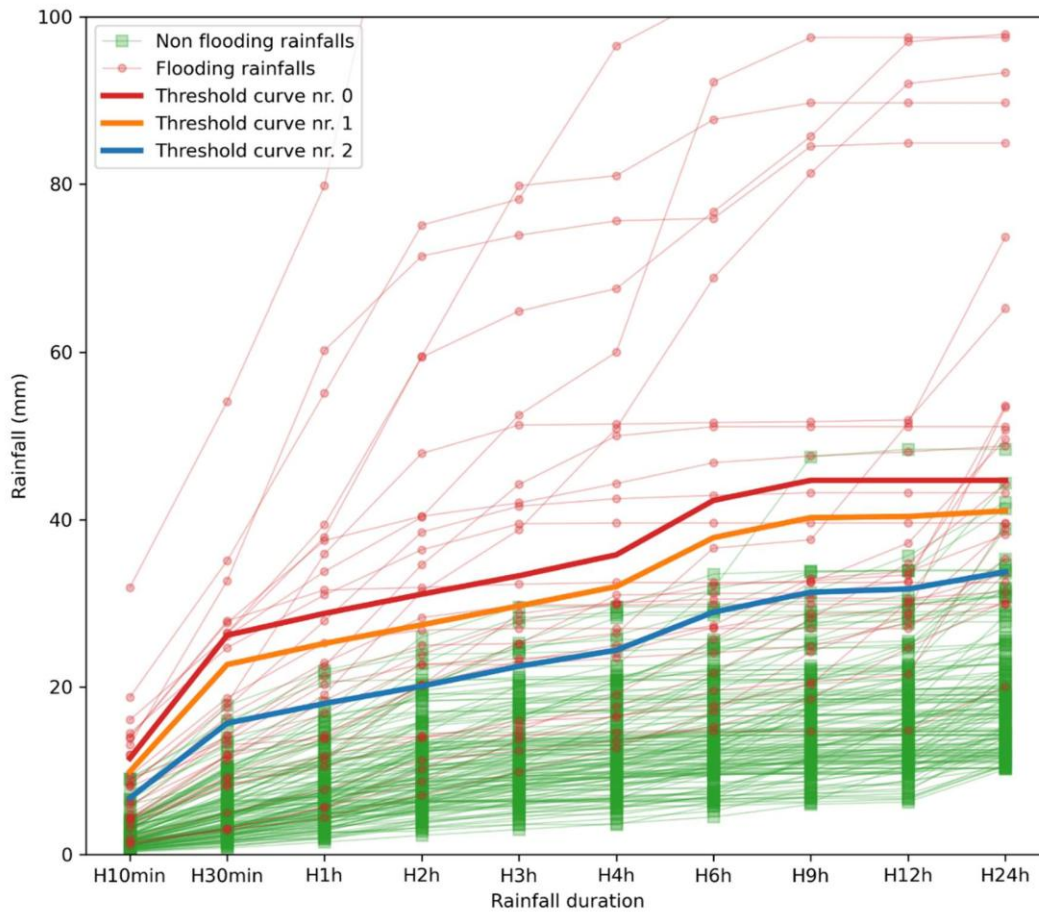


Figure 3.1.2. Flooding and non-flooding depth-duration curves with three best-performing rainfall threshold curves Best-performing rainfall thresholds curves based on 10 features.

3.2 Machine-learning EWS

Machine learning (ML) models were trained and tested using the same dataset as for the threshold model. However, in addition to 10 rainfall features, we also included the daily temperature and three antecedent rainfall conditions. First, we performed a univariate statistical test to select only the best features. Scores of ANOVA F-value test are shown in Figure 3.2.1, which suggests that antecedent rainfall data has almost no impact on flooding, whereas temperature has a much lower effect than the rainfall depths of all durations. Therefore, we dropped the three antecedent condition features and kept the rest (11 features).

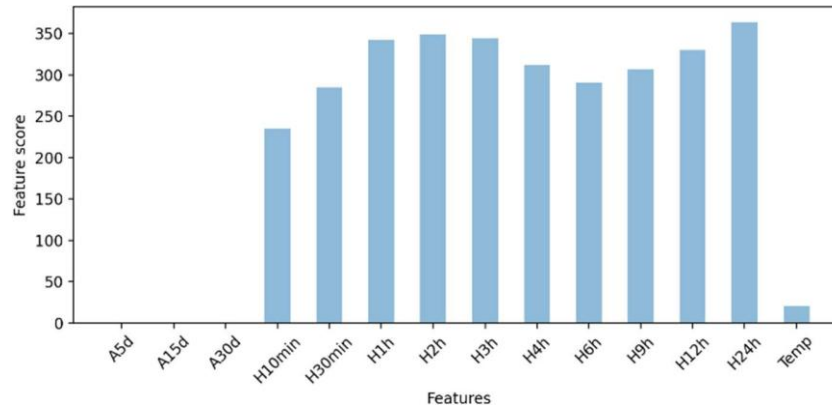


Figure 3.2.1. F-value test scores for all 14 considered features.

After the training step, we evaluated the performance of all 10 ML models using the testing dataset. The confusion matrices from all models are shown in Figures 3.2.2.-3.2.4. and performance indicators are given in Table 3.2.1. The performance of all models based on a combination of ACC and TPR metrics are presented in Figure 3.2.5.

All ML models have an accuracy between 0.89 and 0.95, however, TPR and F1 have a wider range of values. The three best performing ML models are the discriminant analysis (linear and quadratic) and logistic regression (0, 4, and 5). The best model is the quadratic discriminant analysis with an accuracy of 0.95 and F1 score of 0.89. This model had 24 hits (TP), 5 misses (FN) and only 4 false alarms (FP), implying that 83% of flooding events can be accurately predicted using this model.

Table 3.2.1. Performance indicators for ten ML methods based on 11 features

Method	TPR	PPR	ACC	F1	TPR_ACC
0 Logistic regression	0.72	0.99	0.95	0.84	0.69
1 Support vector machine (linear)	0.62	0.99	0.93	0.76	0.58
2 Support vector machine (quadratic)	0.48	0.99	0.91	0.65	0.44
3 Support vector machine (cubic)	0.59	0.99	0.92	0.74	0.54
4 Discriminant analysis (linear)	0.66	0.99	0.94	0.79	0.61
5 Discriminant analysis (quadratic)	0.83	0.97	0.95	0.89	0.78
6 Decision trees, N=8	0.55	0.96	0.89	0.70	0.49
7 Decision trees, N=18	0.69	0.95	0.91	0.80	0.62
8 KNN, Euc. distance, n=3	0.62	0.95	0.89	0.75	0.55
9 KNN, Euc. distance, n=15	0.62	0.99	0.92	0.76	0.57

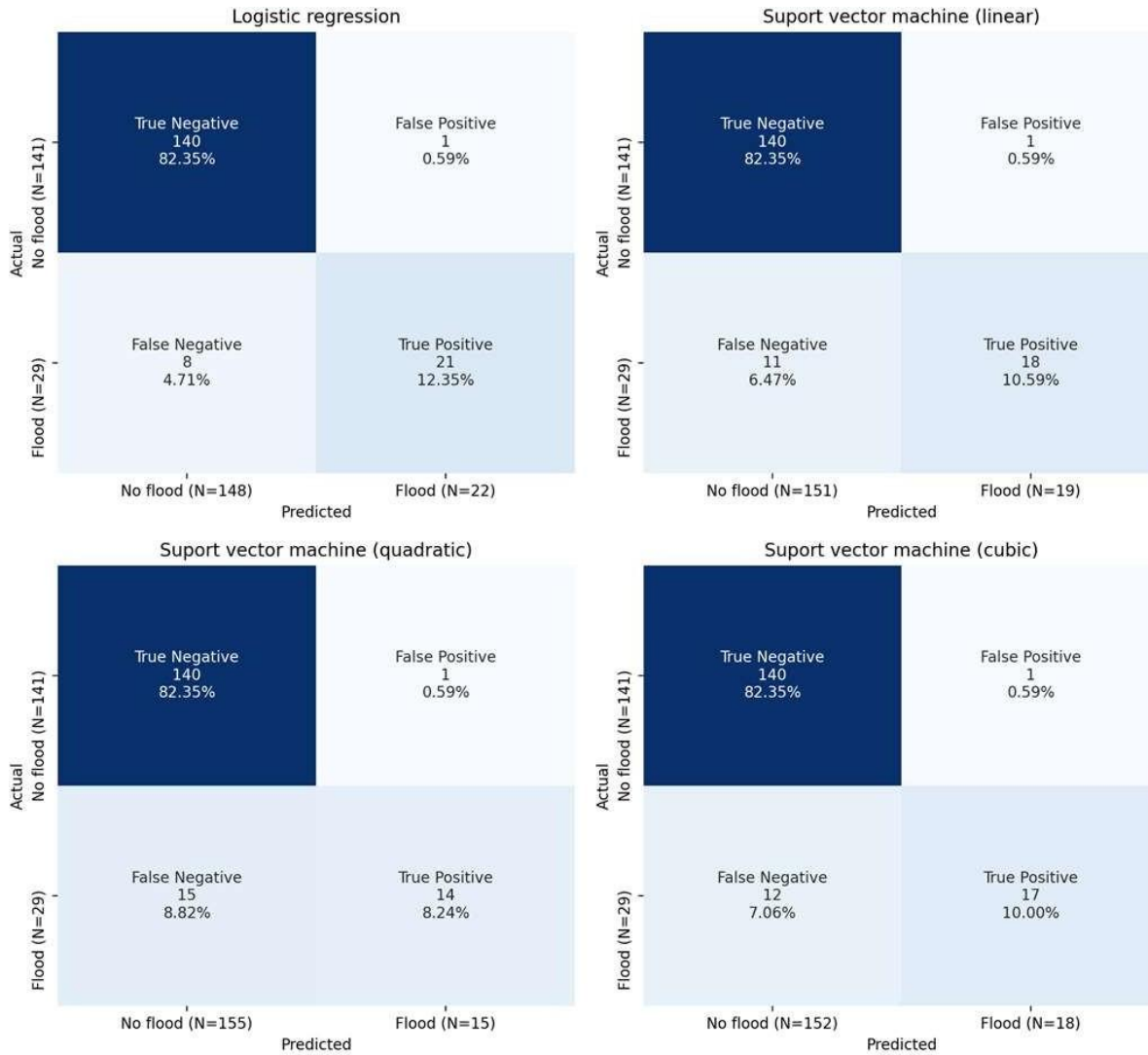


Figure 3.2.2. Confusion matrices for logistic regression, and three support vector machine algorithms based on 11 features.

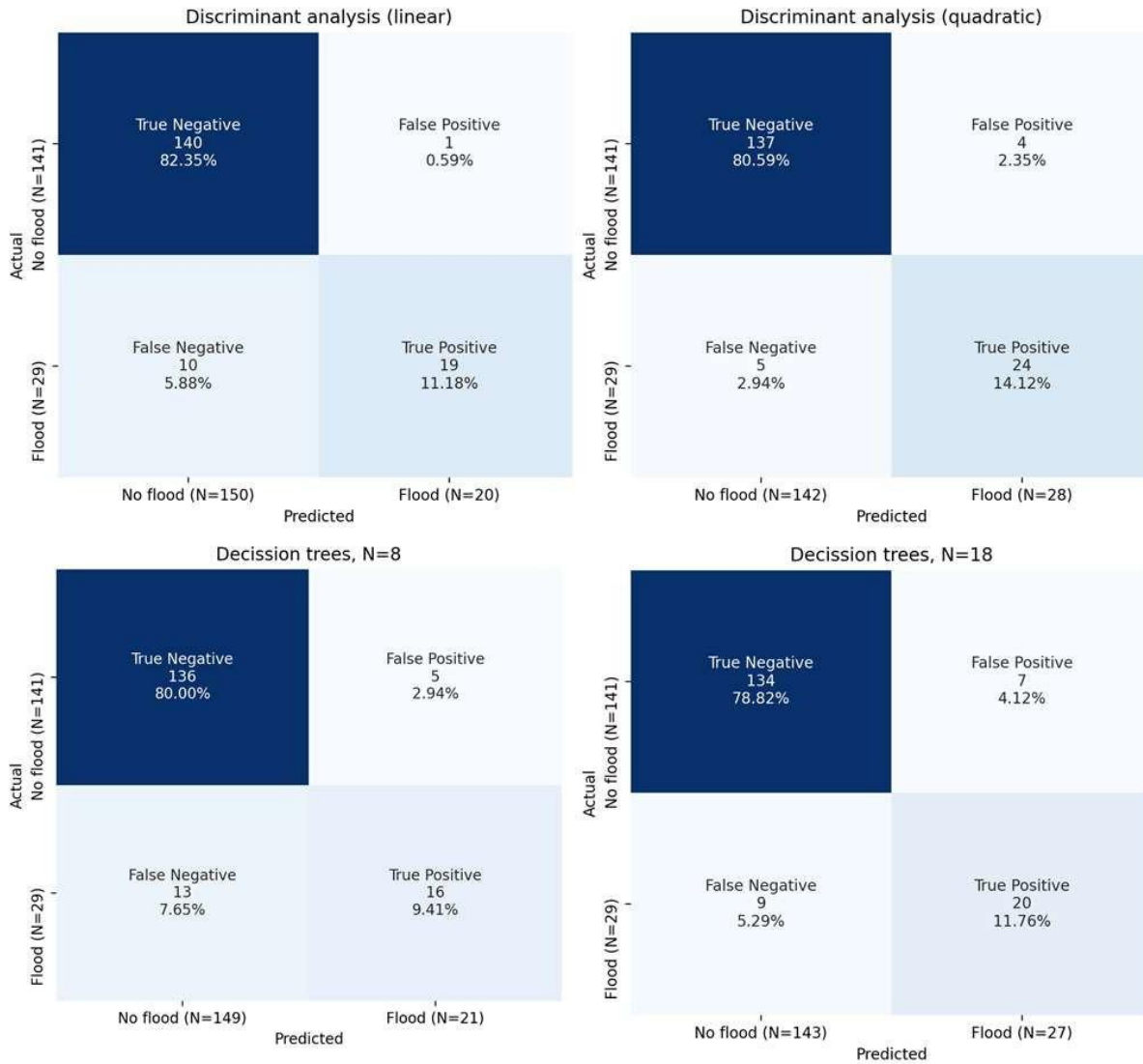


Figure 3.2.3. Confusion matrices for two discriminant analysis and two decision tree algorithms based on 11 features.

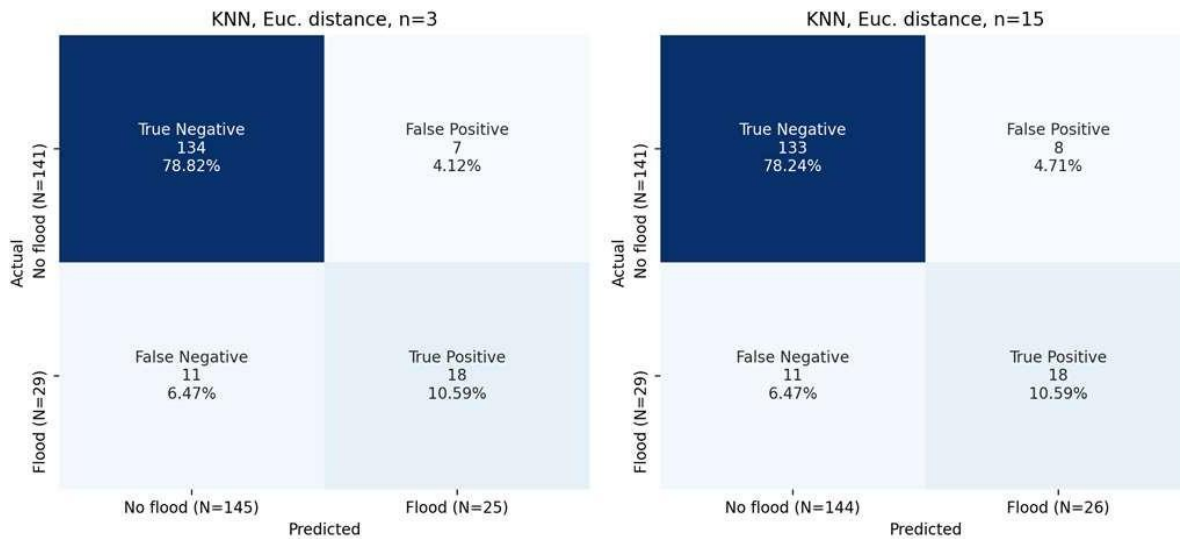


Figure 3.2.4. Confusion matrices for two nearest neighbour algorithms based on 11 features.

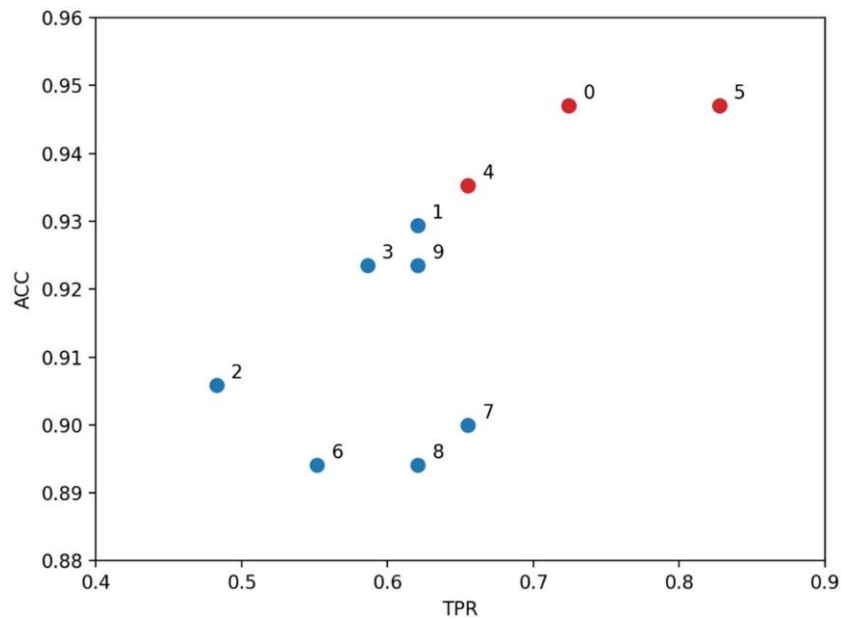


Figure 3.2.5. Model performance of all 10 ML algorithms based on accuracy (ACC) and true predictive rate (TPR) based on 11 features, red colour depicts best performing ML methods.

4 Pluvial flood forecast model

4.1 Threshold-based pluvial flood forecast

Using the same training set as for the EWS model, but with only four features (3-, 6-, 12-, and 24-hour rainfall) we again performed a thorough search for all possible combinations of parameters α , β and γ . From the pool of several thousand combinations, we selected the three best threshold curves, which have the highest value of at least one of the considered metrics. Derived rainfall thresholds for each considered duration (model feature) are shown in Table 4.1.1. These threshold curves were then applied to the testing set and the confusion matrix for each of the three threshold curves is shown in Figure 4.1.1. with the performance indicators presented in Table 4.1.2. Finally, the comparison of testing depth-duration curves (flooding and non-flooding) against three derived threshold curves is illustrated in Figure 4.1.2.

All three curves have an accuracy between 0.84 and 0.93. Similar to the EWS model with 10 features, curve nr. 0 has the highest overall accuracy, but fewer true positive predictions and a high number of the false negative predictions (missed flood events), whereas curve nr. 2 has the highest true positive rate and most true positive predictions, but also a larger number of false positive predictions (false alarms). Curve nr.1 is in between the other two curves with the highest F1 score and balanced false positive and false negative predictions. Overall, these rainfall thresholds derived for only four features have very similar performance metrics as the EWS model, which is more complex to use in practical application.

Table 4.1.1 Best-performing rainfall thresholds curves in (mm) based on 4 features.

Curve	H3h	H6h	H12h	H24h
0	33.3	42.3	44.7	44.7
1	28.5	34.7	38.7	39.2
2	18.8	25.3	29.4	31.4

Table 4.1.2. Best-performing rainfall threshold curve parameters and their performance indicators based on 4 features.

Curve	α	β	γ	TPR	TNR	PPR	NPR	ACC	F1	TPR_ACC
0	0.0	1.0	0.0	0.59	0.99	0.94	0.92	0.92	0.72	0.54
1	0.18	1.0	0.35	0.76	0.96	0.81	0.95	0.93	0.79	0.71
2	0.1	1.0	0.7	0.93	0.82	0.51	0.98	0.84	0.66	0.78

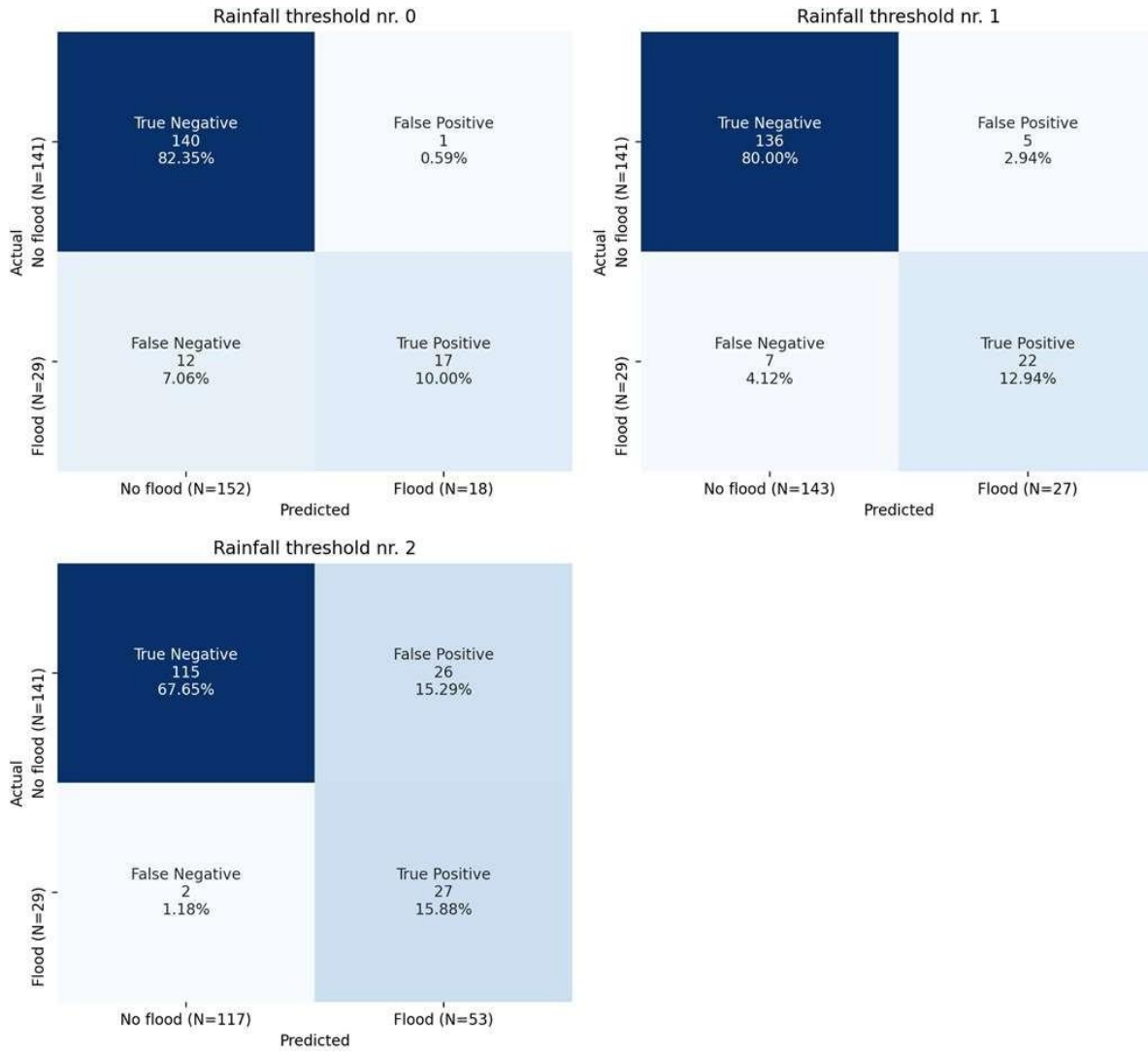


Figure 4.1.1. Confusion matrices for three best performing rainfall threshold curves based on 4 features.

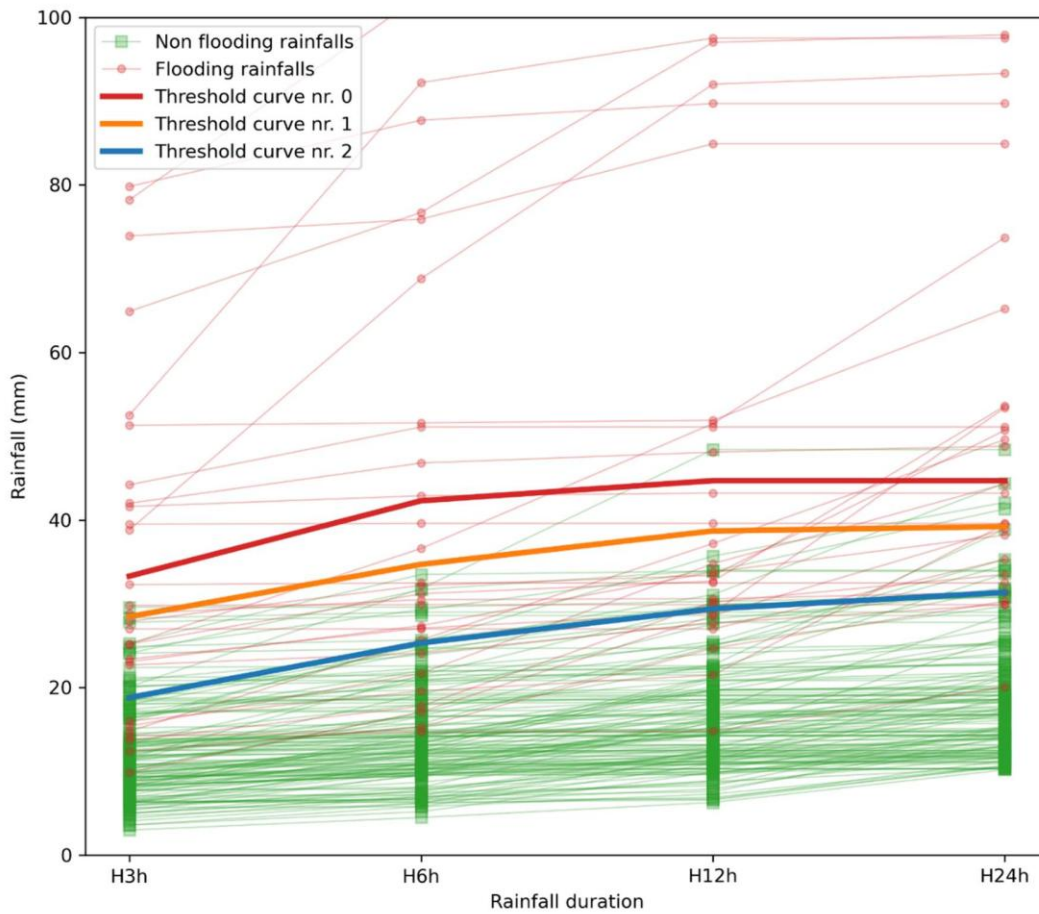


Figure 4.1.2. Flooding and non-flooding depth-duration curves with three best-performing rainfall threshold curves Best-performing rainfall thresholds curves based on 4 features.

4.2 ML-based pluvial flood forecast

Machine learning (ML) models were trained and tested using the same dataset as for the threshold model. However, in contrast to the EWS model based on 11 features the forecast model uses only four features that are publicly available through official weather forecast (ALADIN).

After the training step, we evaluated the performance of all 10 ML models using the testing dataset. The confusion matrices from all models are shown in Figures 4.2.1.-4.2.3. and performance indicators are given in Table 4.2.1. The performance of all models based on a combination of ACC and TPR metrics are presented in Figure 4.2.4.

All ML models have an accuracy between 0.87 and 0.94, which is very close to the EWS model with 11 features. The three best performing ML models are the discriminant analysis (quadratic), logistic regression and k-nearest neighbours (0, 5, and 8). The best model is again the quadratic discriminant analysis with an accuracy of 0.94 and a f1 score of 0.89. This model had 24 hits (TP), 5 misses (FN) and only 5 false alarms (FP), implying that 83% of flooding events can be accurately predicted using this model. This is an almost identical performance as with 11 features.

Table 4.2.1. Performance indicators for ten ML methods based on 4 features.

Method	FN	FP	TN	TP	TPR	PPR	ACC	F1	TPR_ACC
0 Logistic regression	9	2	139	20	0.69	0.99	0.94	0.81	0.65
1 Support vector machine (linear)	14	1	140	15	0.52	0.99	0.91	0.68	0.47
2 Support vector machine (quadratic)	16	0	141	13	0.45	1.00	0.91	0.62	0.41
3 Support vector machine (cubic)	13	1	140	16	0.55	0.99	0.92	0.71	0.51
4 Discriminant analysis (linear)	11	2	139	18	0.62	0.99	0.92	0.76	0.57
5 Discriminant analysis (quadratic)	5	5	136	24	0.83	0.96	0.94	0.89	0.78
6 Decision trees, N=8	16	6	135	13	0.45	0.96	0.87	0.61	0.39
7 Decision trees, N=18	9	12	129	20	0.69	0.91	0.88	0.79	0.60
8 KNN, Euc. distance, n=3	9	4	137	20	0.69	0.97	0.92	0.81	0.64
9 KNN, Euc. distance, n=15	12	2	139	17	0.59	0.99	0.92	0.74	0.54

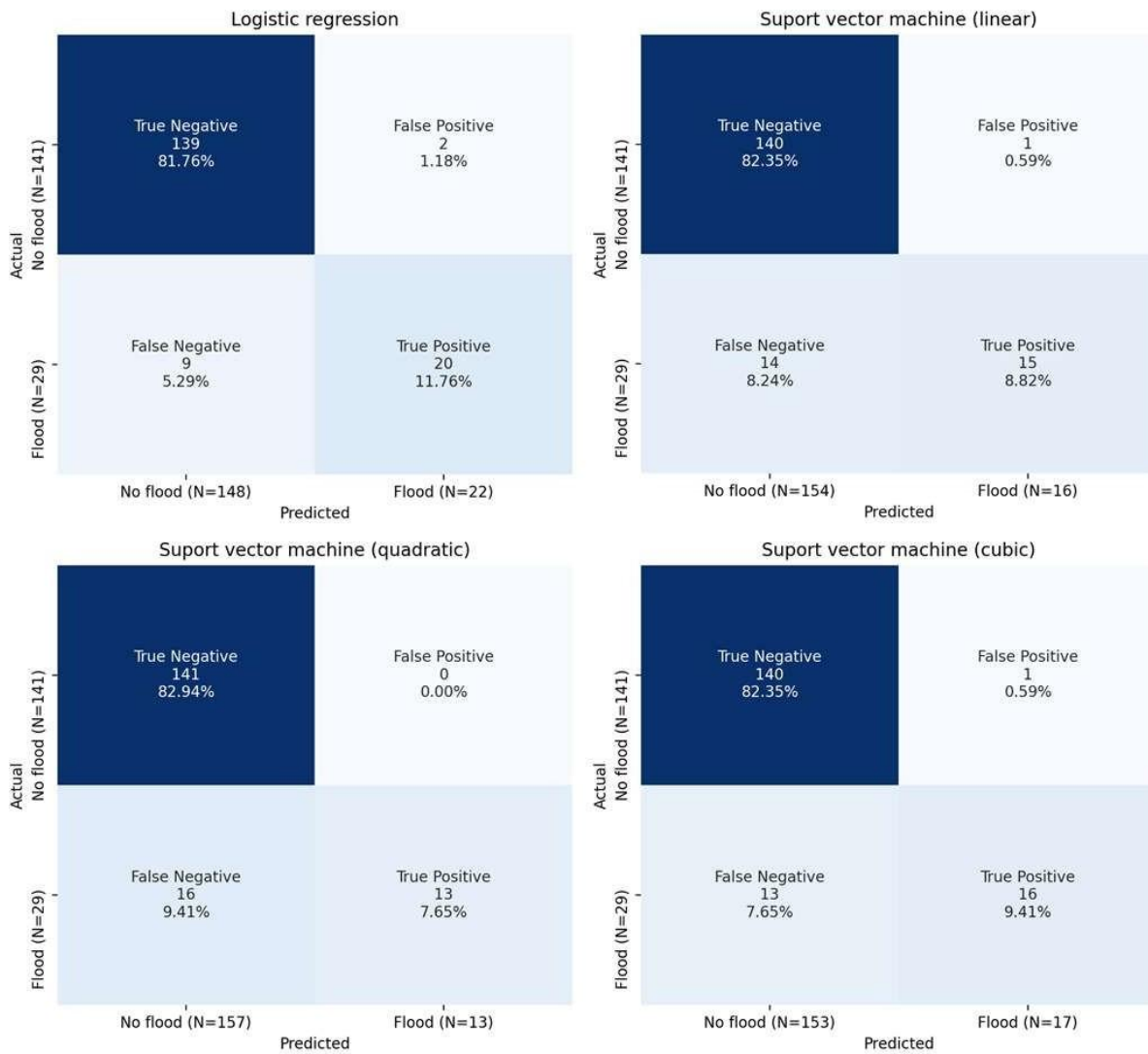


Figure 4.2.1. Confusion matrices for logistic regression, and three support vector machine algorithms based on 4 features.

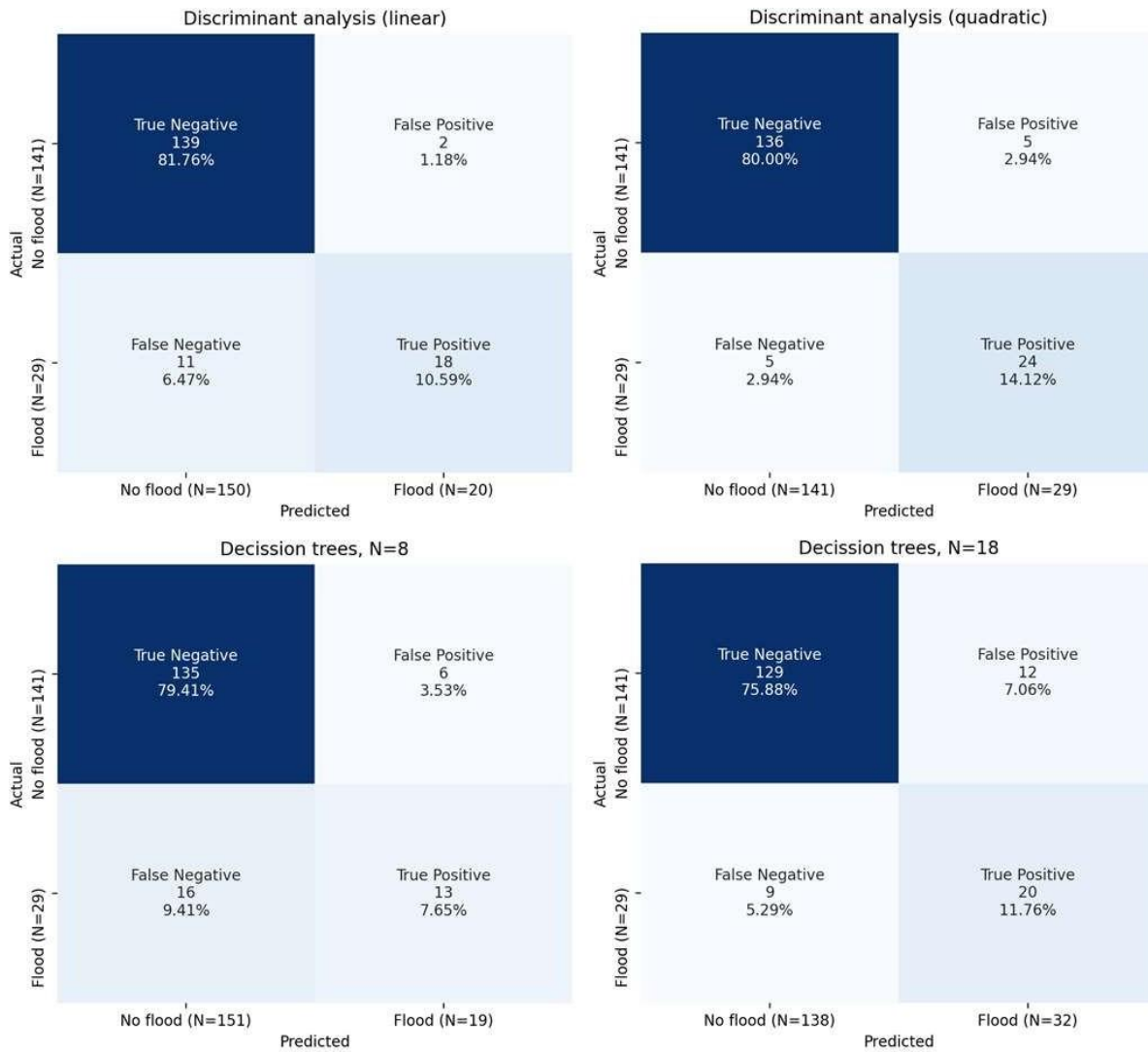


Figure 4.2.2. Confusion matrices for two discriminant analysis and two decision tree algorithms based on 4 features.

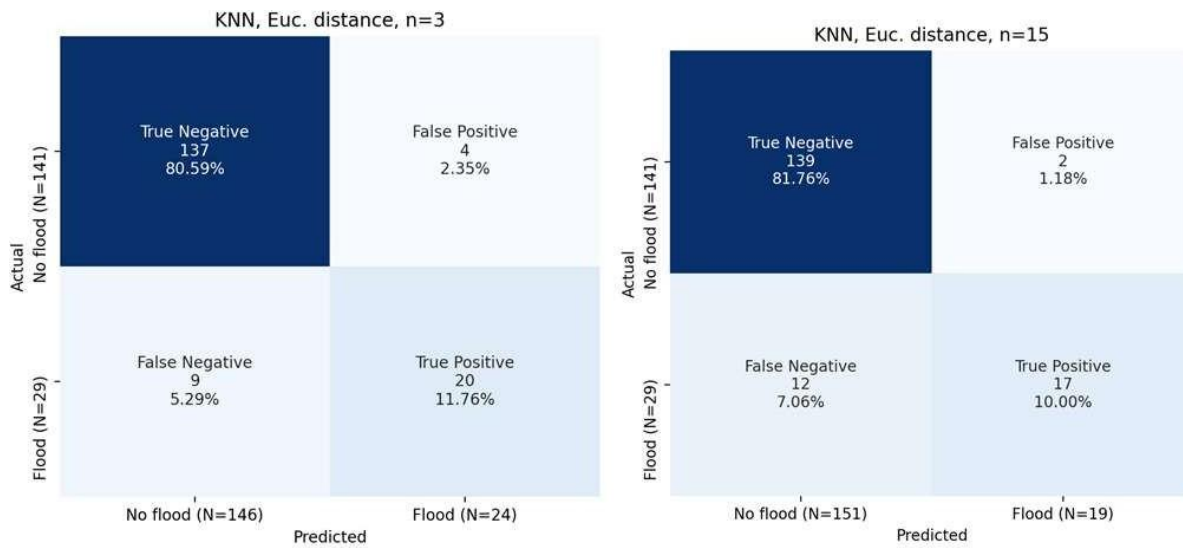


Figure 4.2.3. Confusion matrices for two nearest neighbour algorithms based on 4 features.

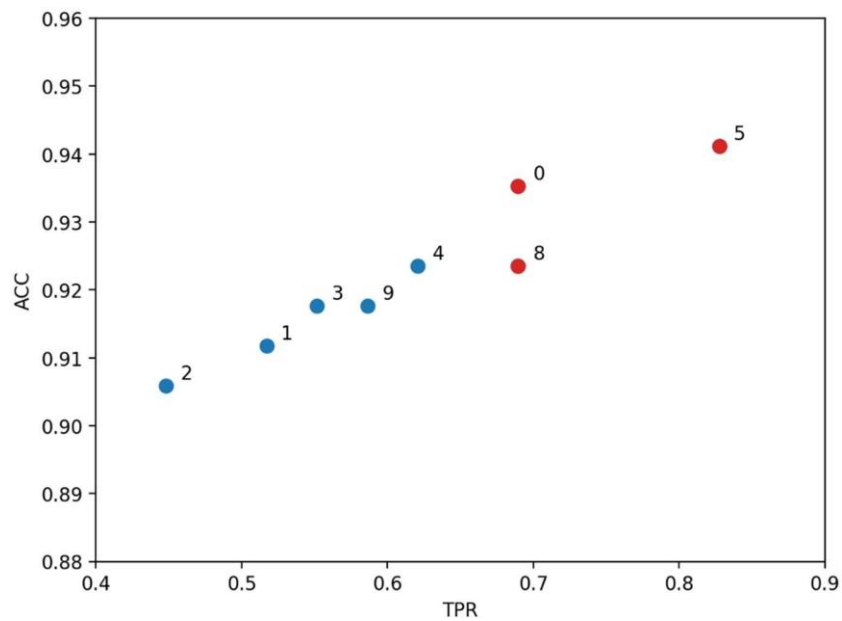


Figure 4.2.4. Model performance of all 10 ML algorithms based on accuracy (ACC) and true predictive rate (TPR) based on 4 features., red colour depicts best performing ML methods.

5 Conclusion

This study has presented the development of a pluvial flood forecast model for the Zadar pilot area. The model is based on 20-years of collected data, consisting of individual news reports on pluvial flooding and continuous 5-min rain gauge data. Two different computational approaches have been considered. The first – conventional one – is based on rainfall threshold curves that define critical rainfall for different durations above which flooding is likely to occur. The second approach is based on machine learning and a classification problem – predicting whether accumulated rainfall depths over different durations will generate pluvial flooding. For the second approach, we have considered 10 different methods belonging to five machine learning categories, which are usually applied for classification problems. Namely, these are logistic regression, support vector machine, discriminant analysis, decision trees, and nearest neighbours.

Furthermore, we have considered two different applications for these predictive models - an early warning system that uses real-time high-resolution rainfall data and a flood forecasting model which uses official weather forecasts from the ALADIN model (publicly available from the Croatian Meteorological and Hydrological Service, DHMZ). For the first purpose, we have trained all models using 10 and 11 features (accumulated rainfall depths over different durations and daily temperature), whereas for the second purpose we have considered only four rainfall depths for durations in 3-hour steps to make them compatible with the ALADIN weather forecast.

After careful analysis, we have defined rainfall threshold curves for the Zadar pilot area which can be used for both an early warning system and flood forecasting system with high accuracy. Some machine learning models can provide slightly more accurate predictions, with the quadratic discriminant analysis being the most successful method for this purpose.

Overall, this study showed that the flood predictions based on news reports can be a reliable approach in the Zadar pilot area. The analysis performed in this study has laid the foundation for the implementation of an early warning system and flood forecast system in Zadar and other pilot areas in Croatia.

Literature

- ALADIN Consortium web page, <http://www.umn-cnrm.fr/aladin/spip.php?article36>, 29-12-2021
- Croatian Meteorological and Hydrological Service, <https://meteo.hr/>, 29-12-2021
- EUMETSAT, Flash floods in Zadar and surrounding areas, <https://www.eumetsat.int/flash-floods-zadar-and-surrounding-areas>, 29-12-2021
- Giannecchini, R., Galanti, Y., & D'Amato Avanzi, G. (2012). Critical rainfall thresholds for triggering shallow landslides in the Serchio River Valley (Tuscany, Italy). *Natural Hazards and Earth System Sciences*, 12(3), 829-842.
- Hong, M., Kim, J., & Jeong, S. (2018). Rainfall intensity-duration thresholds for landslide prediction in South Korea by considering the effects of antecedent rainfall. *Landslides*, 15(3), 523-534.
- Kalin, K. C., Nimac, I., Patalen, L., & Pasaric, Z. (2021). *Spatio-temporal analysis of short-term rainfall extremes in Croatia* (No. EMS2021-311). Copernicus Meetings.
- Ke, Q., Tian, X., Bricker, J., Tian, Z., Guan, G., Cai, H., ... & Liu, J. (2020). Urban pluvial flooding prediction by machine learning approaches—a case study of Shenzhen city, China. *Advances in Water Resources*, 145, 103719.
- Martina, M. L. V., Todini, E., & Libralon, A. (2006). A Bayesian decision approach to rainfall thresholds based flood warning. *Hydrology and earth system sciences*, 10(3), 413-426.
- METEOALARM, <https://meteoalarm.org/>, 29-12-2021
- Oesper, L., Merico, D., Isserlin, R., & Bader, G. D. (2011). WordCloud: a Cytoscape plugin to create a visual semantic summary of networks. *Source Code for Biology and Medicine*, 6(1), 7.
- Pan, H. L., Jiang, Y. J., Wang, J., & Ou, G. Q. (2018). Rainfall threshold calculation for debris flow early warning in areas with scarcity of data. *Natural Hazards and Earth System Sciences*, 18(5), 1395-1409.
- Pedregosa, F., Varoquaux, G., Gramfort, A., Michel, V., Thirion, B., Grisel, O., ... & Duchesnay, E. (2011). Scikit-learn: Machine learning in Python. *the Journal of machine Learning research*, 12, 2825-2830.
- Tian, X., Schleiss, M., Bouwens, C., & van de Giesen, N. (2019). Critical rainfall thresholds for urban pluvial flooding inferred from citizen observations. *Science of the Total Environment*, 689, 258-268.
- WorldPop (www.worldpop.org - School of Geography and Environmental Science, University of Southampton; Department of Geography and Geosciences, University of Louisville; Departement de Geographie, Universite de Namur) and Center for International Earth Science Information Network (CIESIN), Columbia University (2018). Global High Resolution Population Denominators Project - Funded by The Bill and Melinda Gates Foundation (OPP1134076). <https://dx.doi.org/10.5258/SOTON/WP00675>

Yang, T. H., Hwang, G. D., Tsai, C. C., & Ho, J. Y. (2016). Using rainfall thresholds and ensemble precipitation forecasts to issue and improve urban inundation alerts. *Hydrology and Earth System Sciences*, 20(12), 4731-4745.

Zhai, X., Guo, L., Liu, R., & Zhang, Y. (2018). Rainfall threshold determination for flash flood warning in mountainous catchments with consideration of antecedent soil moisture and rainfall pattern. *Natural Hazards*, 94(2), 605-625.